Estuarine, Coastal and Shelf Science 218 (2019) 197–203

Contents lists available at ScienceDirect

Estuarine, Coastal and Shelf Science

journal homepage: www.elsevier.com/locate/ecss

Multi-decadal variability in sandy beach area and the role of climate forcing

Luis Orlando[a,*], Leonardo Ortega[b], Omar Defeo[a]

[a] UNDECIMAR, Facultad de Ciencias, Iguá 4225, Montevideo, 11400, Uruguay
[b] Dirección Nacional de Recursos Acuáticos, Constituyente 1497, Montevideo, 11200, Uruguay

ARTICLE INFO

Keywords:
Beach area
Climatic forcing
ENSO
Erosion
Sea level
Open-access information

ABSTRACT

Sandy beaches comprise 31% of the ice free coasts of the world, providing a variety of ecosystem services essential to support human well-being, particularly protection against erosion and extreme climatic events. These highly dynamic environments are controlled principally by wave energy, tides and grain size, generating complex morphodynamic patterns that translate into strong area variation. Estimates of beach area and its variability are prime inputs for coastal management, a challenge that requires data representing a wide spatiotemporal scale. In this paper, a Landsat-based semi-automated methodology was developed to reconstruct the area of 21 sandy beaches of the Montevideo (Uruguay) coast from 1984 to 2016. This long-term information was also used to discern erosion-accretion cycles by means of wavelet analysis, and to explore the role of climatic forcing on these cycles through linear mixed models. A random forest classification algorithm was applied to Landsat images in order to estimate beach area. Long-term trends described a 27-year cycle with well-delimited quasi-decadal erosion and accretion phases related to climatic configurations. The beach area was negatively affected by an increase in sea level and climatic conditions of the previous year, being positively correlated with sea surface temperature anomalies and offshore winds (which favored accretion) and negatively correlated with onshore winds and intense El Niño Southern Oscillation (ENSO) events (favoring erosion). Our findings, together with the predicted increase in the occurrence and intensity of storms and extreme ENSO events, constitute a worrying scenario, as erosion in this populated coastal zone could have negative social, economic and ecological repercussions. The methodology developed here was useful to detect long-term changes in beach area and is entirely based on open-access information. Therefore, it is potentially applicable at any location on the planet. This approach is also useful to counteract the scarcity of long-term information that has precluded robust assessments of climate change effects on coastal zones.

1. Introduction

Sandy beaches comprise 31% of the ice free coasts of the world (Luijendijk et al., 2018), and provide a wide variety of ecosystem services essential to support human well-being. These services include, among others: sediment storage and associated buffering against extreme events (Short, 1999); water filtration and purification (Constanza et al., 2014); and maintenance of biodiversity and economic development for humans (Defeo et al., 2009). The physical structure of sandy beaches is determined by the interaction between sand, waves and tides (Short, 1999). Sediment transport, in the surf zone by wave action and in the dunes by wind action, promotes an extremely dynamic environment where sand and water are always in motion. From a two-dimensional perspective, this high dynamics translates into strong short-term beach area variations (Short, 1999).

Ecosystem area is a major ecological variable, positively correlated with species diversity, population persistence and food chain length (Schoener, 1989; Takimoto and Post, 2013), and could also impact ecosystem attributes such as resilience (Dunne et al., 2002) and services (Balvanera et al., 2014). In sandy beach ecosystems, studies drawn from a pool of widely differing beaches all around the world have shown a consistent increase in species richness, abundance and biomass of macrofaunal communities as beach width increases (reviewed in McLachlan and Defeo, 2018). It has been also shown that beaches with larger intertidal areas support larger populations, thus reducing the probability of species extirpations (Defeo and McLachlan, 2013; Barboza and Defeo, 2015; Defeo et al., 2017). Therefore, habitat availability, as indicated by beach width, may be important in explaining local to regional variations in sandy beach diversity patterns. Stressors that affect beach area also impact over ecosystem attributes, especially those associated with resilience to natural hazards (Defeo et al., 2009), seriously undermining human well-being in areas where

* Corresponding author.
E-mail address: lorlandoch@gmail.com (L. Orlando).

https://doi.org/10.1016/j.ecss.2018.12.015
Received 17 September 2018; Received in revised form 4 December 2018; Accepted 24 December 2018
Available online 28 December 2018
0272-7714/

population density is nearly three times higher than the global average (Small and Nicholls, 2003).

Coasts are undergoing increasing use by human populations worldwide, characterized by an intensification of urban development (Defeo et al., 2009). Sandy beaches are particularly vulnerable to physical modifications derived from sand mining, armoring structures and urban-associated alterations, which reduce the ecosystem area and alter sediment budget and cycles, thus accelerating erosion rates (Short, 1999; Torres et al., 2017). Global climate change, particularly sea-level rise and increased storm frequency, has added a new dimension to worldwide modifications of shorelines (McLachlan and Defeo, 2018). In this context of climatic and human stressors converging on coasts, 24% of the world's sandy beaches are persistently eroding (Luijendijk et al., 2018).

Estimations of beach area and its temporal variability are prime inputs for coastal management (Short and Jackson, 2013); a challenge that requires data representing a wide range of spatial and temporal scales (Barnard et al., 2012). Coastal monitoring on-site programs provide insights on coastal dynamics (Harley et al., 2010), but are expensive and often temporally and spatially sparse (Splinter et al., 2013). This is especially problematic, as robust long-term data sets are required before meaningful trends emerge (Harley et al., 2010). Therefore, several information sources for shoreline analysis and beach area estimation have been explored to complement on-site surveys (Short and Jackson, 2013). Among them, aerial photographs provide excellent spatial coverage of beach systems, but are heavily limited in their time and geographic coverage (Short and Jackson, 2013). Satellite imagery has been highlighted as the most realistic way forward in providing useful data for studies of nearshore morphodynamics (Harris et al., 2011; Short and Jackson, 2013) and has been widely used for shoreline and coastal monitoring at global (Luijendijk et al., 2018) and local (Harris et al., 2011; Ozturk and Sesli, 2015) scales. Landsat satellite series have spatial, spectral, and radiometric resolution and, along with their temporal continuity, have proven well-suited for land characterization activities (Ozturk and Sesli, 2015, Luijendijk et al., 2018).

Montevideo city hosts approximately 45% of the total population of Uruguay, with the most conspicuous residential areas, industries and services (e.g. oil refinery, port, recreational areas) concentrated within its coastal zone (Saizar, 1997). Besides its ecological and economic importance, the coast is the most iconic public space and an integral part of Montevidean identity and daily life. Due to its recreational use, natural characteristics, architectural values, ethnical links to immigrant culture and even spiritual connotations, it has been proposed as a World Heritage site (UNESCO, 2010). However, the Uruguayan coast and its sandy beaches have been increasingly affected by climate change stressors, including sea-level rise (Fig. 1b) and warmer sea waters (Fig. 1c), which have been accompanied by flooding/drought events and an increase in the frequency of storms and in the frequency and intensity of onshore winds (Ortega et al., 2013; Barreiro, 2017). Altogether, these stressors could affect sandy beach ecosystems, which can be perceived as ecosystems at risk. There is thus a need to increase knowledge on long-term sandy beach dynamics, including variations in erosion and accretion phases and their relationship with climate forcing (Barnard et al., 2015).

Semi-automated classification of information has been extensively applied on remote sensing studies as a way to map different ecosystems land cover at local and global levels (Millard and Richardson, 2015; Hansen et al., 2013). This methodology requires reference training areas for the classifying algorithm to map the categories on the region of interest (Millard and Richardson, 2015). In this paper, a Landsat-based semi-automated methodology was developed to reconstruct the area of 21 sandy beaches of the Montevideo coast from 1984 to 2016. This long-term information is also used to discern erosion-accretion cycles by means of wavelet analysis, and to explore the role of climatic forcing on these cycles through linear mixed models.

2. Methods

2.1. Study site

The Montevideo coast (Fig. 1) is characterized by sandy beaches interrupted by rocky heads, with a semidiurnal tidal regime with microtidal amplitude (ca. 0.5 m). However, strong onshore winds produce unpredictable short-term increases in sea level (storm surges up to 4 m) (Lercari and Defeo, 2006). The Rio de la Plata has a major freshwater input from Parana and Uruguay rivers, forming a shallow (up to 15 m) coastal-plain estuary (Lercari and Defeo, 2006). A strong turbidity front is located around Montevideo city, which constitutes the surface indication of the transition between fresh and saline waters (Sepúlveda et al., 2004). In this estuary, variability of water characteristics (salinity, temperature and turbidity) is mainly forced by winds (Simionato et al., 2010).

2.2. Beach area estimation

Beach area was estimated from 1984 to 2016 for 21 beaches of the Montevideo coast (Fig. 1S, Supplementary Material). Almost all beaches included in this study are southern-oriented (10 towards the S, 5 to SE, 5 to SW and 1 to W) (following Engstrom, 1973). Google Earth Engine (GEE) open platform for satellite image processing (Gorelick et al., 2017) and associated satellite collections were used. Beaches were measured using all the available standard Level 1 Terrain-corrected orthorectified images from Landsat 5 (L5) (1984–2011) and Landsat 7 (L7) (2004–2016). All satellite information was restricted to a 20-km radius of coordinates 34°52′12″S, 56°13′48″W (Fig. 1a). L5 had an average of 15 images per year with a minimum of 6 (1985) and a maximum of 31 (2004), while L7 had an average of 32 images per year with a minimum of 28 (2010) and a maximum of 38 (2011). Landsat images were converted to top of the atmosphere reflectance to remove the effect of clouds and shadows (Luijendijk et al., 2018). A median-based annual composite was constructed from the non-cloudy pixels and used to estimate beach area. In order to improve the accuracy of beach area estimates, the water layer was removed by applying a normalized difference water index (NDWI) mask (Gao, 1996), combined with photo interpretation. Polygons enclosing each of the 21 beaches were constructed based on Quickbird satellite images from Google Earth (2.5 m spatial resolution), and used to obtain individual measures for each beach. A random forest supervised classification algorithm was applied to distinguish sand from other kinds of cover (e.g., rocky, hard structures, vegetation), the 7 (8) spectral bands of Landsat 5 (7) were considered as classification variables (Cutler et al., 2007). For the sand category, training polygons were distributed along the coast, and sand areas were interpreted from imagery and relocated for each year composite to deal with variations on shoreline position and image characteristics. The category “other” was formed by polygons that comprised all non-sand cover, including urban, rocky, rural and vegetation cover. For each category, 100 training points were randomly extracted from the training areas, considering that: 1) the number of training points should be at least ten times the number of variables used in the classification (Jensen, 2005); and 2) random selection of points within training areas reduces spatial autocorrelation and classification errors (Millard and Richardson, 2015). As sand only represents 0.01% of the total surface in the study region, collecting proportionally more training data can enable a better representation of the statistical characteristics and variability of these proportionately-smaller classes, even though it may lead to over-representation (Millard and Richardson, 2015). In order to override this factor and provide a better characterization of the sand category optical properties, the threshold of the majority vote to determine the predicted class of every pixel was increased to 65% of the predictions for sand observations. Following this procedure, 1000 decision trees were constructed for each year. All pixels within the beach polygons and classified as “other” with a

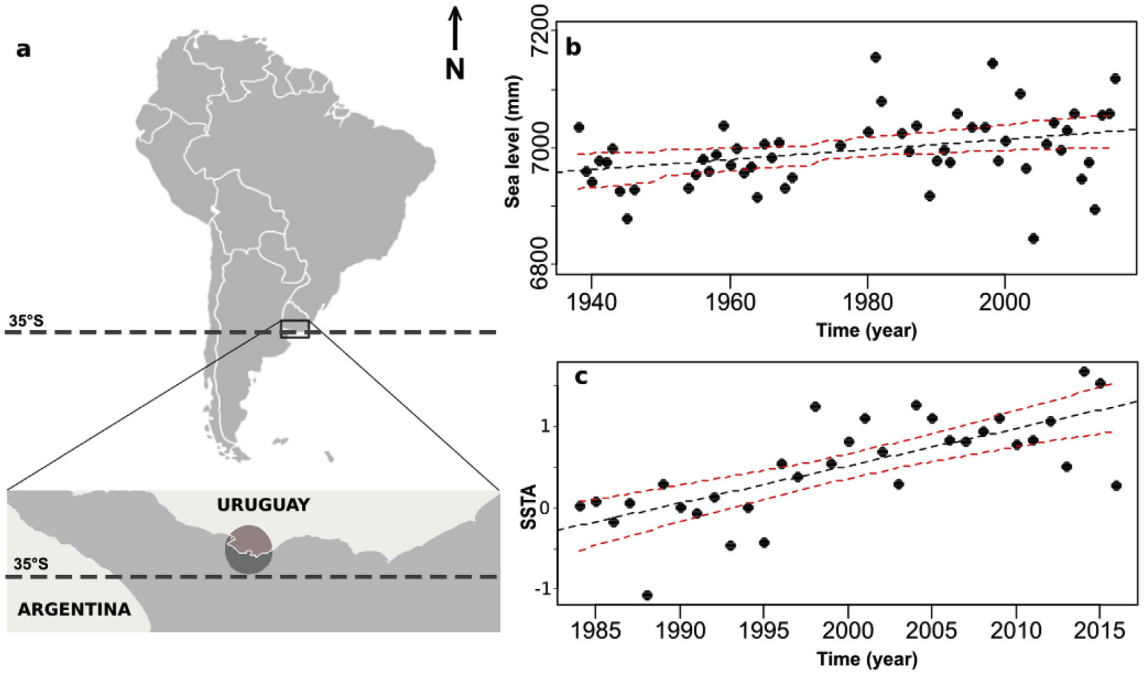

Fig. 1. a) Study area, with the circle in the lower panel highlighting a 20-km radius area that includes the coast of Montevideo where this study was focused. Long-term trends with linear models and 95% confidence intervals in b) annual mean sea level in Montevideo ($y = 0.875x + 5263.1$, $R^2 = 0.12$); and c) yearly sea surface temperature anomalies (SSTA) for the region (40W-60W/30S-40S) ($y = 0.046x - 91.261$, $R^2 = 0.51$). Both trends are highly significant ($p < 0.01$).

Table 1
Summary of climatic variables used in this study, detailing units, a general description and information source.

Variable	Units	Description
Meridional Wind	m/s	Annual mean of monthly meridional winds for the region (40W-60W/30S-40S)
Zonal Wind	m/s	Annual mean of monthly zonal winds for the region (40W-60W/30S-40S)
Wind direction	Degrees	Direction of resultant wind from Zonal and Meridional
Wind velocity	m/s	Speed of resultant wind from Zonal and Meridional
Categorical wind direction	Categorical	Categorization of wind direction in 8 groups (N, NE, E, …)
Sea level Montevideo	mm	Level of the sea measured in the Montevideo Port
Global Sea level	mm	Global level of the sea
Precipitation anomaly in Montevideo	mm	Anomaly of precipitations in Montevideo
Precipitation anomaly in the de la Plata river basin	mm	Anomaly of precipitations at the Rio de la Plata basin
Atmospheric temperature	°C	Anomaly of temperature at 2 m of altitude (40°W-60°W/30°S-40°S)
Sea surface temperature anomaly (SSTA)	°C	Anomaly of sea surface temperature (40°W-60°W/30°S-40°S)
Uruguay river flow anomaly	m^3/s	Anomaly of water flow from Salto Grande Hydrological power plant
Rio de la Plata flow anomaly	m^3/s	Anomaly of water flow from Instituto Nacional del Agua y el Ambiente
ENSO 3.4	Continuous	SSTA based index for determining Niño/Niña events and intensity
ENSO	Categorical	ONI based classification of years as Niño, Niña or neutral, and intensity
Pacific Decadal Oscillation (PDO)	Continuous	Yearly average of PDO monthly values
Atlantic Multidecadal Oscillation (AMO)	Continuous	Yearly average of AMO monthly values

normalized difference vegetation index > 0, were considered as beach vegetation and added to the total beach area. To allow comparisons between beaches with different sizes, the normalized beach area was calculated as the standard score for each beach (standard score (i) = (i-mean)/standard deviation), and will be referred as beach area hereafter.

2.3. Wavelet and coherence analysis

Wavelet transform is a well-suited tool for the study of non-stationary processes occurring over finite spatial and temporal domains (Lau and Weng, 1995) and has been applied to analyze temporal patterns of beach erosion (Short and Trembanis, 2004). By decomposing a time series into a time-frequency space, it is possible to determine both the dominant modes of variability and their variation through time (Torrence and Compo, 1998). In order to evaluate significant cyclic behavior in beach area and to determine its frequency, a wavelet analysis was applied using the "dog" mother wavelet (Short and Trembanis, 2004). Coherence analysis was performed to complement wavelets by measuring the cross-correlation of two time series as a function of frequency (Torrence and Compo, 1998), which can be interpreted as a decomposition of the correlation coefficient at a different scales, i.e., the local correlation between time series in a time-frequency space (Casagrande et al., 2015). This analysis reveals the interaction between different processes at different scales, and points out which variable leads over the other. Coherence analysis was applied to beach area against El Niño Southern Oscillation (ENSO) 3.4 index, Atlantic Multidecadal oscillation (AMO) and the Pacific Decadal Oscillation (PDO) index, using the "morlet" mother wavelet (Torrence and Compo, 1998). All wavelet and coherence analyses were made using the *biwavelet* package (R Development Core Team, 2012).

2.4. Climatic information and modeling procedure

In order to assess the relationships between beach area estimations and climate, annual averages of climatic variables linked to beach erosion/accretion (Short, 1999), and those relevant for the region (Ortega et al., 2013) were gathered (Table 1). Yearly-average sea surface temperature anomalies (SSTA) were estimated from a 1° × 1° latitude, longitude resolution grid and five wind variables were assessed: meridional and zonal wind velocity (IRI/LDEO, Reynolds et al., 2002; Kalnay et al., 1996), and the resultant wind direction and speed and categorized wind direction (CWD) in 8 orientations (N, NE, E, SE, S, SW, W, NW). Two measures of sea level were included, one local and one global (GLOSS, Bradshaw et al., 2015). Temperature was considered at 2 m high in the atmosphere and in the sea surface (NCEP-NCAR, Kistler et al., 2001). As precipitation and river flow have been linked with sea level and erosive patterns in the Uruguayan coast (Saizar, 1997), precipitations at site and in the Rio de la Plata basin (PERSIANN CDR, Sorooshian et al., 2014) were included. River flow estimates for the Rio Uruguay and Rio de la Plata (Borus et al., 2017) were also included. To represent general climatic patterns, global climatic indices were considered: the PDO continuous index (NCEI/NOAA, Mantua and Hare, 2002), the AMO index (NOAA/NCEP, Enfield et al., 2001) and the ENSO 3.4 continuous index (NOAA/NCEP CPC, Trenberth, 1997). Changes in the PDO and AMO tend to coincide with changes in the relative frequency of ENSO events affecting precipitations, SST and atmospheric patterns in the study region (Andreoli and Kayano, 2005; Verdon and Franks, 2006). ENSO 3.4 has shown the highest correlation with precipitations, SST and atmospheric pressure anomalies on the South Atlantic (Colberg et al., 2004). Also, an ENSO categorical index based on the Oceanic Niño Index (ONI) was included, with events defined as 3 consecutive overlapping 3-month periods at or above the +0.5° anomaly for warm (El Niño) events and at or below the −0.5 anomaly for cold (La Niña) events. This threshold was further broken down into Weak (with a 0.5 to 0.9 SSTA), Moderate (1.0–1.4), Strong (1.5–1.9) and Very Strong (≥2.0) events (GGWS, Null, 2018).

Linear mixed models were used for modeling the relationship between beach area and climatic variables. To assess long-term trends in erosion-accretion patterns in the Montevideo coast, the normalized areas of each of the 21 beaches were taken as replicates within each year. The incorporation of random effects allowed us to combine variations in annual climatic configuration with direct effect variables acting on beach area (Bolker et al., 2009). The categorical ENSO variable was included as random intercept in order to summarize possible effects on beach area related to different ENSO conditions. Pearson's correlation coefficient was applied to discard redundant variables, and then linear mixed models were started with different combinations of variables and refined by dropping non-significant variables, until models including all significant variables were accomplished. Akaike's Information Criterion (AIC) was applied to evaluate each model's fit and parsimony, as well as for selecting the best model. All climatic variables were modelled with and without a 1-year time lag, on the understanding that current beach area is the result of a temporal integration of forcing factors. For the random intercept, lag-levels were determined through coherence analysis. Linear modeling assumptions were tested (Bolker et al., 2009) and modeling procedures were performed applying the *lmer* package of R.

3. Results

A total of 693 measures were obtained from 21 beaches over a 33-year period (1984–2016) (Fig. 2a). Beach area showed a cyclic long-term pattern with phases of accretion (positive beach area variation) and erosion (negative beach area variation). Global wavelet spectrum showed a significant dominant periodicity of 27 years (Fig. 2b), which is consistent with the observed multidecadal cycle in the beach area (Fig. 2a). Wavelet variance of beach area decreased through time, following the cycle of accretion/erosion transitions (Fig. 2c). Coherence analysis showed a statistically significant relationship between the ENSO 3.4 index and beach area at periods of 1–3.5 years between 1997 and 2003, where beach area lags ENSO (Fig. 2S, Supplementary Material). No significant relationships were found between beach area and the multidecadal climatic indexes, PDO and AMO.

The best fit model for beach area (Table 2, Fig. 3) included a negative effect of sea level (Fig. 3b), a positive effect of SSTA recorded in the previous year (Fig. 3c) and an effect of 1-year lagged categorical wind direction. The positive effect over beach area was associated with northerly winds, while winds with a south component had a negative effect (Fig. 3d). One-year lagged Categorical ENSO showed the best results, with an overall negative effect on beach area (Fig. 3e). Only weak La Niña years showed a positive influence on beach area, with erosive effects increasing with the intensity of the events.

4. Discussion

Long-term trends in sandy beach area at Montevideo described a 27-year cycle, with well-delimited quasi-decadal erosion and accretion phases related with climatic configurations. The modeling process selected simultaneous and lagged annual variables to explain long-term patterns in beach area. The statistically significant relationships between beach area and current (e.g., sea level) and past (1-year lagged mean wind direction, SSTA and ENSO index) forcing conditions reinforce the notion that drivers acting at different time scales are co-responsible for the present and future behavior of sediment budget in sandy beaches (Short, 1999). It also highlights the role of the past climate forcing in erosion/accretion cycles.

The methodology developed here was useful to detect long-term changes in beach area and is entirely based on open-access information. Therefore, it is potentially applicable at any location on the planet, particularly in those regions where the regional wave climate genesis, tidal regime, and sediment transport regimes are comparable. This approach could be used to counteract the scarcity of long-term information that has precluded robust assessments of climate change effects on coastal zones (Harley et al., 2010; Harris et al., 2011; Short and Jackson, 2013; Splinter et al., 2013). However, its implementation should be conducted with caution, particularly in cases of differences in effective Landsat coverage (which could vary according to location). Close collaboration with local sandy beach researchers is strongly emphasized. In general, satellite-based studies of coastal behavior are mainly directed to determine the position of the water/sand interface and are mainly focused on erosion rates (Ozturk and Sesli, 2015; Luijendijk et al., 2018). In this context, the methodological approach developed here was useful to reconstruct information on coastal behavior and, at the same time, allowed for the detection of sand and vegetation areas within the beach, as well as their distribution in space and time, a feature with relevant potential for ecological studies and conservation and management programs. Indeed, the approach could also be useful to determine the area of planning units (beaches), and to integrate information from different beaches on a large scale to assess variations in sand budget and ecosystem quality, which in turn could be critical to determine reserve networks directed to sustain biodiversity (Margules and Pressey, 2000). In addition, the methodology is suitable to help ensure the sustainability of ecosystem services associated with sandy shores (Harris et al., 2011). Different management actions should be incorporated in the modeling process, taking into account that changes to beaches and dunes due to both unplanned and planned human actions (e.g., nourishment, engineering structures such as groins, revetments and breakwaters) are increasing exponentially, reducing sediment supply and therefore altering beach area.

The positive relationship between beach area and lagged SSTA could be explained by the integrated role of wind patterns, oceanic circulation, precipitations and solar insolation (Simionato et al., 2010), that took place the year before. Therefore, SSTA could be considered as

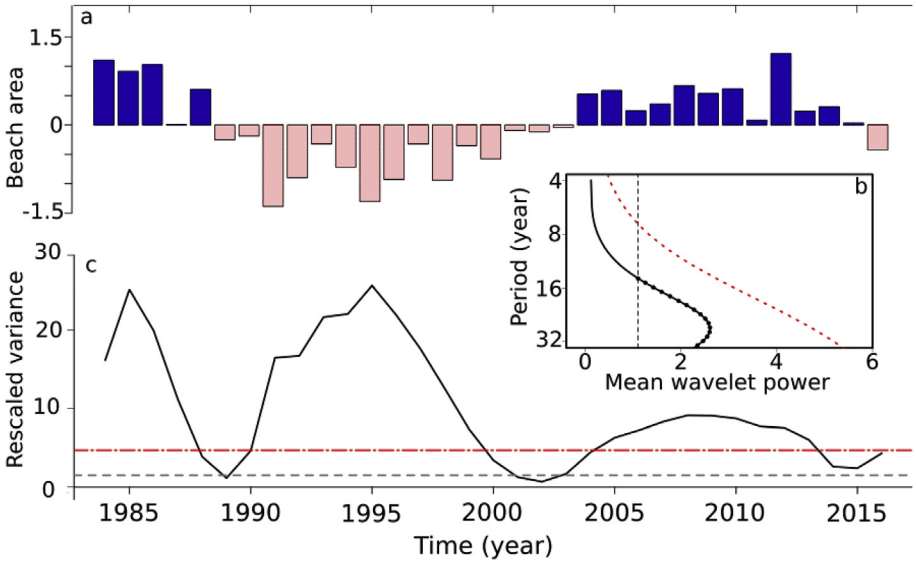

Fig. 2. Wavelet analysis. a) Annual median normalized beach area over the study period (1984–2016). b) Global wavelet spectrum: the vertical dashed line is the white noise threshold, the curved dashed line is the red noise threshold, and the mean wavelet power (variance) is the continuous black line with significant periods represented by dots. c) Scaled average power (mean variance) in time (solid line). The red dot-dash line represents 95% red noise threshold and the grey dashed line shows 95% white noise threshold. (For interpretation of the references to colour in this figure legend, the reader is referred to the Web version of this article.)

Table 2
Linear mixed models adjusted for predicting normalized beach area. Fixed effect variables and random effects variables on the model intercept are listed for each model. **d.f.**: degrees of freedom, **AIC**: Akaike information criterion, $\mathbf{R^2m}$ marginal R^2, $\mathbf{R^2c}$ conditional R^2. Sea level was measured at Montevideo Port; wind was categorized in eight directions; SSTA: sea surface temperature anomaly; ENSO: El Niño Southern Oscillation, discriminated by category according to phase and intensity; RdlP: Rio de la Plata; PDO: Pacific Decadal Oscillation index; "*lag*" indicates 1-year lagged variable.

#	Fixed effects	Random effect	d.f.	AIC	R^2m	R^2c
1	sea level + categorized wind direction *lag* + SSTA *lag*	ENSO *lag*	12	1858	0.18	0.40
2	sea level + meridional wind *lag* + SSTA *lag*	ENSO *lag*	6	1868	0.10	0.20
3	categorized wind direction *lag* + SSTA *lag* + RdlP flow *lag*	ENSO *lag*	12	1886	0.17	0.44
4	meridional wind *lag* + SSTA *lag* + RdlP flow	ENSO *lag*	6	1890	0.10	0.17
5	Uruguay flow *lag* + meridional wind *lag* + SSTA *lag* + PDO lag	ENSO *lag*	7	1903	0.11	0.23

an aggregate variable that carries different simultaneous effects of the previous year general conditions in current beach state. Higher SSTA values are associated with warm calm conditions in the study area (Simionato et al., 2010) that favor accretion of beaches, whereas lower SSTA has been associated with strong onshore winds (Alves and Pezzuto, 2009) that produce high-energy waves inducing erosion. This is in agreement with the negative effects of southerly wind on beach area estimated by the linear mixed model (Fig. 3d) and the Montevideo coast orientation, which is mainly south-facing (Fig. 1). Offshore (north) winds pushes the water away from the coast and decrease wave energy, favoring accretion, whereas onshore (south) winds increases the aerial loss of sediment to the land and wave energy, also pushing the water over the beach, resulting in augmented erosion rates. Wind direction is therefore an important explanatory variable in the evolution and orientation of coastal features (Bauer et al., 2012), and its effects on beach area can be ascribed to aerial erosion and a modulation of wave energy.

The ENSO signal influences SSTA and air temperature in the region, generating complex climatic configurations that modify precipitation and wind patterns (Barreiro, 2010) and therefore altering beach area. The increase of northerly winds during El Niño (Barreiro, 2017) has been invoked to explain an increase of beach area in the region (Gutiérrez et al., 2016). However, increasing precipitation levels and storm occurrence with El Niño intensity resulted in increased erosion (Fig. 3e). Higher incidence of strong winds from the south quadrant during La Niña (Barreiro, 2017) also increased erosion. However, there is a decrease in precipitations after weak La Niña events, and the erosion by wind is likely to be compensated by calm climatic conditions that favor accretion (Gutiérrez et al., 2016) (Fig. 3e). In that vein, the period between 1998 and 2002 was characterized by a dominance of weak and moderate La Niña (Null, 2018), when beach area tended to increase, followed by a shift to a positive accretion phase.

The erosion/accretion patterns in Montevideo beaches responded to physical forcing and changing climatic conditions, supporting the shared concern about the potentially critical effects of climate change in coastal areas (Barnard et al., 2015). The sea surface temperature of the South Atlantic Ocean is expected to increase linearly at a decadal scale (Fei-Fei et al., 2012). A doubling in the frequency of extreme El Niño events, followed by extreme La Niña, has been predicted (Cai et al., 2015), with potentially negative effects on sandy beaches in the region. According to the modeling results presented here, the enhanced intensity and frequency of ENSO events, together with sea level rise and increased storminess, constitute a highly erosive scenario for the Montevideo coast. This has utmost importance, taking into account that this coast is influenced by waters of the Southwestern Atlantic Ocean, a major global hotspot where warming occurs at several times the average global rate (Hobday and Pecl, 2014). Indeed, the warm front in this region, as indicated by the 20 °C isotherm, showed a consistent long-term poleward shift at a rate of 9 km yr^{-1} and coastal air temperatures in the region are also warming (Ortega et al., 2016).

In summary, the modeling approach selected global (ENSO) and regional (SSTA) climatic indices, in combination with wind direction (a proxy for wave energy and direction) and sea level as relevant correlates of beach area. The set of selected variables has a similar structure to the findings of Barnard et al. (2015) for the Pacific Ocean basin, where climatic indices, wave energy flux, wave direction, and sea level anomalies were strongly related to coastal response. The positive long-term relationship between temperature (i.e., SSTA) and sea level, together with the occurrence of more frequent and severe storms resulting from warmer air and sea temperatures (Fig. 1c) is threatening Montevideo beaches and could increase erosion rates, a trend already observed in sandy beaches of the Atlantic coast of Uruguay (Ortega et al.,

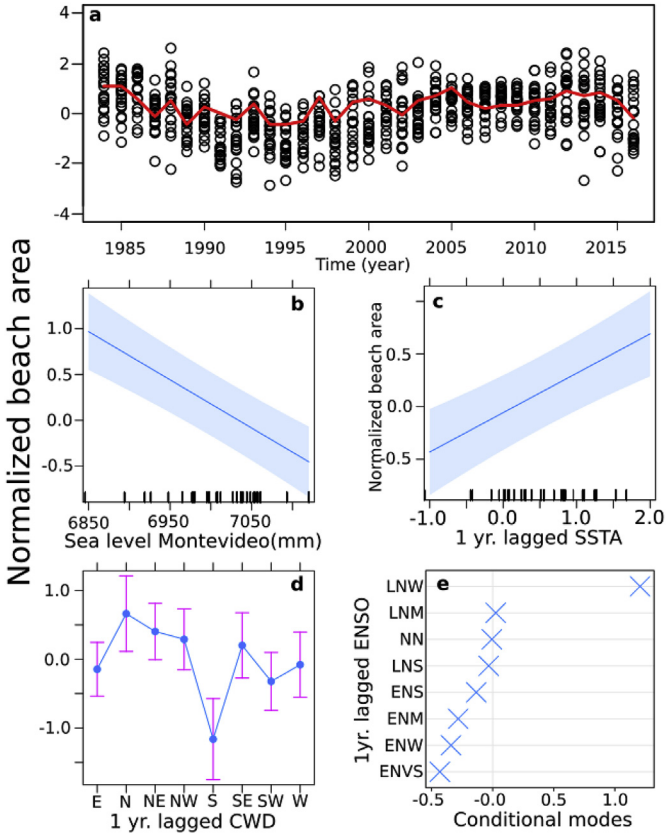

Fig. 3. Normalized beach area variations between 1984 and 2016 and best linear mixed model fitted. a) Scatterplot showing the normalized area for each beach and year, with the continuous red line indicating the best model prediction. Effect plots of: b) Montevideo sea level, c) 1-year lagged sea surface temperature anomaly (SSTA), and d) 1-year lagged categorical wind direction (CWD) on normalized beach area. e) Conditional modes for different ENSO conditions with 1-year lag: La Niña Weak (LNW), El Niño Weak (ENW), Neutral (NN), El Niño Strong (ENS), La Niña Strong (LNS), La Niña Moderate (LNM), El Niño Moderate (ENM) and El Niño Very Strong (ENVS). (For interpretation of the references to colour in this figure legend, the reader is referred to the Web version of this article.)

2013). The inverse relationship between sea level and beach area reinforces the notion that the major long-term threat facing sandy beaches worldwide is coastal squeeze (Pontee, 2013), which leaves beaches trapped between rising sea level on the wet side and encroaching development from expanding human populations on land, thus leaving no space for normal sediment dynamics (McLachlan and Defeo, 2018).

Coastal erosion in Montevideo sandy beaches is affecting highly relevant ecological and socioeconomic values (Saizar, 1997; UNESCO, 2010; Gutiérrez et al., 2016). These social-ecological systems (McLachlan and Defeo, 2018) are important for recreation and biodiversity conservation, and therefore should attend a hierarchy of concerns related to public safety, economy and ecology (McLachlan et al., 2013; Elliott et al., 2016). In this context, reconstructing beach area information following the approach developed here could provide insights on ecosystem recovery scenarios and could help outline appropriate management strategies with multiple objectives in these social-ecological systems, particularly in erosive scenarios that require active recovery (Elliott et al., 2007; McLachlan and Defeo, 2018). The restoration of suitable physical conditions will allow system recovery, which in turn will increase ecosystem services and resilience (Balvanera et al., 2014). Furthermore, knowing the climate forcing factors would help predict beach area evolution under different climate change scenarios and also identify key variables for recovery. However, the social-ecological dimensions of beach area loss remain under-explored, as there are no baselines of ecological (e.g., ecosystem services) and economic (e.g., recreation value) indicators for these sandy beaches. Thus, a continued assessment of the effects of climate change should be given a high priority in conservation planning for this coastal region.

Acknowledgements

This work is part of Luis Orlando PhD thesis and has been kindly supported by the project Variability of Ocean Ecosystems Around South America (VOCES) through a research grant (CRN3070) from the Inter-American Institute for Global Change Research. Support has also been provided by PEDECIBA and CSIC Grupos (32). We would like to thank the UNDECIMAR group for valuable discussions and the two anonymous referees for their constructive comments.

Appendix A. Supplementary data

Supplementary data to this article can be found online at https://doi.org/10.1016/j.ecss.2018.12.015.

References

Alves, E.S., Pezzuto, P.R., 2009. Effect of cold fronts on the benthic macrofauna of exposed sandy beaches with contrasting morphodynamics. Braz. J. Oceanogr. 57, 73–96.
Andreoli, R.V., Kayano, M.T., 2005. ENSO-related rainfall anomalies in South America and associated circulation features during warm and cold Pacific decadal oscillation regimes. Int. J. Climatol. 25, 2017–2030.
Balvanera, P., Siddique, I., Dee, L., Paquette, A., Isbell, F., Gonzalez, A., Byrnes, J., O'Connor, M.I., Hungate, B.A., Griffin, J.N., 2014. Linking biodiversity and ecosystem services: current uncertainties and the necessary next steps. Bioscience 64, 49–57.
Barboza, F.R., Defeo, O., 2015. Global diversity patterns in sandy beach macrofauna: a biogeographic analysis. Sci. Rep. 5, 14515.
Barnard, P.L., Hubbard, D.M., Dugan, J.E., 2012. Beach response dynamics of a littoral cell using a 17-year single-point time series of sand thickness. Geomorphology 139–140, 588–598.
Barnard, P.L., Short, A.D., Harley, M.D., Splinter, K.D., Vitousek, S., Turner, I.L., Allan, J., Banno, M., Bryan, K.R., Doria, A., Hansen, J.E., Kato, S., Kuriyama, Y., Randall-Goodwin, E., Ruggiero, P., Walker, I.J., Heathfield, D.K., 2015. Coastal vulnerability across the Pacific dominated by El niño/southern oscillation. Nat. Geosci. 8, 801–808.
Barreiro, M., 2010. Influence of ENSO and the south Atlantic Ocean on climate predictability over southeastern south America. Clim. Dynam. 35, 1493–1508.
Barreiro, M., 2017. Interannual variability of extratropical transient wave activity and its influence on rainfall over Uruguay. Int. J. Climatol. 37, 4261–4274.
Bauer, B.O., Davidson-Arnott, R.G.D., Walker, I.J., Hesp, P.A., Ollerhead, J., 2012. Wind direction and complex sediment transport response across a beach–dune system. Earth Surf. Process. Landforms 37, 1661–1677.
Bolker, B.M., Brooks, M.E., Clark, C.J., Geange, S.W., Poulsen, J.R., Stevens, M.H.H., White, J.S.S., 2009. Generalized linear mixed models: a practical guide for ecology and evolution. Trends Ecol. Evol. 24, 127–135.
Borús, J., Uriburu, M., Quirno-Calvo, D., 2017. Evaluación de caudales mensuales descargados por los grandes ríos del sistema del plata al estuario del río de la plata. Alerta Hidrológico - Instituto Nacional del Agua y el Ambiente, Ezeiza, Argentina.
Bradshaw, E., Rickards, L., Aarup, T., 2015. sea level data archaeology and the global sea level observing system (GLOSS). Geo. Res. J. 6, 9–16.
Cai, W., Wang, G., Santoso, A., McPhaden, M.J., Wu, L., Jin, F., Timmermann, A., Collins, M., Vecchi, G., Lengaigne, M., England, M.H., Dommenget, D., Takahashi, K., Guilyardi, E., 2015. Increased frequency of extreme La Niña events under greenhouse warming. Nat. Clim. Change 5, 132.
Casagrande, E., Mueller, B., Miralles, D.G., Entekhabi, D., Molini, A., 2015. Wavelet correlations to reveal multiscale coupling in geophysical systems. J. Geophys. Res. Atmosphere 120, 7555–7572.
Colberg, F., Reason, C.J.C., Rodgers, K., 2004. South Atlantic response to El Niño–Southern Oscillation induced climate variability in an ocean general circulation model. J. Geophys. Res.: Oceans 109.
Costanza, R., de Groot, R., Sutton, P., van der Ploeg, S., Anderson, S.J., Kubiszewski, I., Farber, S., Turner, R.K., 2014. Changes in the global value of ecosystem services. Global Environ. Change 26, 152–158.
Cutler, D.R., Edwards Thomas, C., Beard Karen, H., Cutler, Adele, Hess Kyle, T., Gibson, J., Lawler, J.J., 2007. Random forests for classification in Ecology. Ecology 88, 2783–2792.
Defeo, O., McLachlan, A., 2013. Global patterns in sandy beach macrofauna: species richness, abundance, biomass and body size. Geomorphology 199, 106–114.
Defeo, O., McLachlan, A., Schoeman, D.S., Schlacher, T.A., Dugan, J., Jones, A., Lastra, M., Scapini, F., 2009. Threats to sandy beach ecosystems: a review. Estuar. Coast Shelf Sci. 81, 1–12.
Defeo, O., Barboza, C.A.M., Barboza, F.R., Aeberhard, W.H., Cabrini, T.M.B., Cardoso, R.S., Ortega, L., Skinner, V., Worm, B., 2017. Aggregate patterns of macrofaunal

diversity: an interocean comparison. Global Ecol. Biogeogr. 26, 823–834.
Dunne, J.A., Williams, R.J., Martinez, N.D., 2002. Network structure and biodiversity loss in food webs: robustness increases with connectance. Ecol. Lett. 5, 558–567.
Elliott, M., Burdon, D., Hemingway, K.L., Apitz, S.E., 2007. Estuarine, coastal and marine ecosystem restoration: confusing management and science – a revision of concepts. Estuar. Coast Shelf Sci. 74, 349–366.
Elliott, M., Mander, L., Mazik, K., Simenstad, C., Valesini, F., Whitfield, A., Wolanski, E., 2016. Ecoengineering with ecohydrology: successes and failures in estuarine restoration. Estuar. Coast Shelf Sci. 176, 12–35.
Enfield, D.B., Mestas-Nunez, A.M., Trimble, P.J., 2001. The Atlantic Multidecadal Oscillation and its relationship to rainfall and river flows in the continental U.S. Geophys. Res. Lett. 28, 2077–2080.
Engstrom, E., 1973. A method of predicting beach orientation. Prof. Geogr. 25, 12–15.
Fei-Fei, L., Shuanglin, L., Yong-Qi, G., Furevik, T., 2012. A new method for predicting the decadal component of global SST. Atmos. Ocean. Sci. Lett. 5, 521–526.
Gao, B., 1996. NDWI—a normalized difference water index for remote sensing of vegetation liquid water from space. Remote Sens. Environ. 58, 257–266.
Gorelick, N., Hancher, M., Dixon, M., Ilyushchenko, S., Thau, D., Moore, R., 2017. Google Earth engine: planetary-scale geospatial analysis for everyone. Remote Sens. Environ. 202, 18–27.
Gutiérrez, O., Panario, D., Nagy, G.J., Bidegain, M., Montes, C., 2016. Climate teleconnections and indicators of coastal systems response. Ocean Coast Manag. 122, 64–76.
Hansen, M.C., Potapov, P.V., Moore, R., Hancher, M., Turubanova, S.A., Tyukavina, A., Thau, D., Stehman, S.V., Goetz, S.J., Loveland, T.R., Kommareddy, A., Egorov, A., Chini, L., Justice, C.O., Townshend, J.R.G., 2013. High-resolution global maps of 21st-century forest cover change. Science 342, 850.
Harley, M.D., Turner, I.L., Short, A.D., Ranasinghe, R., 2010. Assessment and integration of conventional, RTK-GPS and image-derived beach survey methods for daily to decadal coastal monitoring. Coast. Eng. 58, 194–205.
Harris, L., Nel, R., Schoeman, D., 2011. Mapping beach morphodynamics remotely: a novel application tested on South African sandy shores. Estuar. Coast Shelf Sci. 92, 78–89.
Hobday, A.J., Pecl, G.T., 2014. Identification of global marine hotspots: sentinels for change and vanguards for adaptation action. Rev. Fish Biol. Fish. 24, 415–425.
Jensen, J.R., 2005. Introductory Digital Image Processing, third ed. Prentice Hall, Upper Saddle River, New Jersey.
Kalnay, E., Kanamitsu, M., Kistler, R., Collins, W., Deaven, D., Gandin, L., Iredell, M., Saha, S., White, G., Woollen, J., Zhu, Y., Chelliah, M., Ebisuzaki, W., Higgins, W., Janowiak, J., Mo, K.C., Ropelewski, C., Wang, J., Leetmaa, A., Reynolds, R., Jenne, R., Joseph, D., 1996. The NCEP/NCAR 40-year reanalysis project. Bull. Am. Meteorol. Soc. 77, 437–472.
Kistler, R., Kalnay, E., Collins, W., Saha, S., White, G., Woollen, J., Chelliah, M., Ebisuzaki, W., Kanamitsu, M., Kousky, V., van den Dool, H., Jenne, R., Fiorino, M., 2001. The NCEP–NCAR 50-year reanalysis: monthly means CD-ROM and documentation. Bull. Am. Meteorol. Soc. 82, 247–268.
Lau, K.M., Weng, H., 1995. Climate signal detection using wavelet transform: how to make a time series sing. Bull. Am. Meteorol. Soc. 76, 2391–2402.
Lercari, D., Defeo, O., 2006. Large-scale diversity and abundance trends in sandy beach macrofauna along full gradients of salinity and morphodynamics. Estuar. Coast Shelf Sci. 68, 27–35.
Luijendijk, A., Hagenaars, G., Ranasinghe, R., Baart, F., Donchyts, G., Aarninkhof, S., 2018. The state of the world's beaches. Sci. Rep. 8, 6641.
Mantua, N.J., Hare, S.R., 2002. The Pacific decadal oscillation. J. Oceanogr. 58, 35–44.
Margules, C.R., Pressey, R.L., 2000. Systematic conservation planning. Nature 405, 243.
McLachlan, A., Defeo, O., Jaramillo, E., Short, A., 2013. Sandy beach conservation and recreation: guidelines for optimising management strategies for multi-purpose use. Ocean Coast Manag. 71, 256–268.
McLachlan, A., Defeo, O., 2018. The Ecology of Sandy Shores, third ed. Academic Press, London.
Millard, K., Richardson, M., 2015. On the importance of training data sample selection in random forest image classification: a case study in Peatland ecosystem mapping. Rem. Sens. 7, 8489–8515.
Null, J., 2018. El Niño and La Niña years and intensities. Available at: http://ggweather.com/enso/oni.htm, Accessed date: 2 February 2018.
Ortega, L., Celentano, E., Finkl, C., Defeo, O., 2013. Effects of climate variability on the morphodynamics of Uruguayan sandy beaches. J. Coast Res. 747–755.
Ortega, L., Celentano, E., Delgado, E., Defeo, O., 2016. Climate change influences on abundance, individual size and body abnormalities in a sandy beach clam. Mar. Ecol. Prog. Ser. 545, 203–213.
Ozturk, D., Sesli, F., 2015. Shoreline change analysis of the Kizilirmak Lagoon series. Ocean Coast Manag. 118, 290–308.
Pontee, N., 2013. Defining coastal squeeze: a discussion. Ocean Coast Manag. 84, 204–207.
R Development Core Team, 2012. R: a Language and Environment for Statistical Computing. R Foundation for Statistical Computing, Vienna Available from: http://www.r-project.org/, Accessed date: 30 September 2013.
Reynolds, R.W., Rayner, N.A., Smith, T.M., Stokes, D.C., Wang, W., 2002. An improved in situ and satellite SST analysis for climate. J. Clim. 15, 1609–1625.
Saizar, A., 1997. Assessment of impacts of a potential sea-level rise on the coast of Montevideo, Uruguay. Clim. Res. 9, 73–79.
Schoener, T.W., 1989. Food webs from the small to the large: the Robert H. MacArthur award lecture. Ecology 70, 1559–1589.
Sepúlveda, H.H., Valle-Levinson, A., Framiñan, M.B., 2004. Observations of subtidal and tidal flow in the Río de la Plata Estuary. Cont. Shelf Res. 24, 509–525.
Short, A.D., 1999. Handbook of Beach and Shoreface Morphodynamics. Wiley and Sons, Chichester.
Short, A.D., Jackson, D.W.T., 2013. Beach morphodynamics. In: In: Shroder, J.F. (Ed.), Treatise in Geomorphology. Coastal Geomorphology, vol. 10. Academic Press, San Diego, pp. 106–129.
Short, A.D., Trembanis, A.C., 2004. Decadal scale patterns in beach oscillation and rotation narrabeen beach, Australia—time series, PCA and wavelet analysis. J. Coast Res. 523–532.
Simionato, C.G., Clara Tejedor, M.L., Campetella, C., Guerrero, R., Moreira, D., 2010. Patterns of sea surface temperature variability on seasonal to sub-annual scales at and offshore the Río de la Plata estuary. Cont. Shelf Res. 30, 1983–1997.
Small, C., Nicholls, R.J., 2003. A global analysis of human settlement in coastal zones. J. Coast Res. 19, 584–599.
Sorooshian, S., Hsu, K., Braithwaite, D., Ashouri, H., NOAA CDR Program, 2014. NOAA Climate Data Record (CDR) of Precipitation Estimation from Remotely Sensed Information Using Artificial Neural Networks (PERSIANN-CDR), Version 1 Revision 1. NOAA National Centers for Environmental Information.
Splinter, K.D., Turner, I.L., Davidson, M.A., 2013. How much data is enough? The importance of morphological sampling interval and duration for calibration of empirical shoreline models. Coast. Eng. 77, 14–27.
Takimoto, G., Post, D.M., 2013. Environmental determinants of food-chain length: a meta-analysis. Ecol. Res. 28, 675–681.
Torrence, C., Compo, G.P., 1998. A practical guide to wavelet analysis. Bull. Am. Meteorol. Soc. 79, 61–78.
Torres, A., Brandt, J., Lear, K., Liu, J., 2017. A looming tragedy of the sand commons. Science 357, 970.
Trenberth, K.E., 1997. The definition of El Niño. Bull. Am. Meteorol. Soc. 78, 2771–2778.
UNESCO, 2010. The rambla of the city of Montevideo. Permanent Uruguayan delegation at UNESCO. Available at: http://whc.unesco.org/en/tentativelists/5594, Accessed date: 7 September 2018.
Verdon, D.C., Franks, S.W., 2006. Long-term behaviour of ENSO: interactions with the PDO over the past 400 years inferred from paleoclimate records. Geophys. Res. Lett. 33.